Appl. Phys. B 80, 889–896 (2005)
DOI: 10.1007/s00340-005-1799-0

Applied Physics B
Lasers and Optics

Y.H. CHEN[1,✉]
Y.C. HUANG[2]
Y.Y. LIN[2]
Y.F. CHEN[3]

Intracavity PPLN crystals for ultra-low-voltage laser Q-switching and high-efficiency wavelength conversion

[1]Institute of Optical Sciences, National Central University, Jhongli 320, Taiwan
[2]Department of Electrical Engineering, National Tsing-Hua University, Hsinchu 300, Taiwan
[3]Department of Electro-physics, National Chiaotung University, Hsinchu 300, Taiwan

Received: 27 July 2004 /
Revised version: 9 March 2005
Published online: 22 April 2005 •

ABSTRACT We report to the best of our knowledge the lowest switching voltage in an electro-optically Q-switched Nd:YVO_4 laser by using a 13-mm long, 14-μm-period PPLN crystal as a Pockels cell. A switching voltage as low as ∼ 50 V in the PPLN crystal was sufficient to hold off the lasing of the Q-switched laser at a pump power more than two times above its continuous-wave threshold. When the PPLN Q-switch was driven by a 100-V voltage at 6.5 kHz, we obtained 0.9-kW laser peak power from this 1-W diode-pumped Nd:YVO_4 laser system with 13% output coupling. When the PPLN Pockels cell was cascaded with a 5-cm long, 30-μm-period PPLN crystal, we produced ∼ μJ/pulse energy at 1.59 μm from optical parametric generation inside the actively Q-switched laser.

PACS 42.60.Gd; 42.65.Yj; 42.70.Mp

1 Introduction

A Q-switched laser is capable of generating a high laser peak power. Recent developments in actively and passively Q-switched diode-pumped microchip lasers [1–3] have greatly reduced the cost and size of Q-switched lasers for many applications. An all-solid-state passively Q-switched (PQS) laser employing a saturable absorber integrated with a laser gain medium is particularly simple and compact. Compared to a passively Q-switched laser, an actively Q-switched laser usually has a high power-handling ability and flexibility in Q-switch timing control. However, the advantages associated with an actively Q-switched laser are accompanied with the additional cost and complexity in the Q-switch drive. Among active Q-switching techniques, electro-optic (E-O) Q-switching [1, 2] is known to be advantageous over acousto-optic (A-O) Q-switching [4] in its faster switching time and better hold-off ability, which together result in higher peak power at the laser output. However, most Pockels-cell Q-switches including several recently reported E-O Q-switches [1, 2, 5] required a high-voltage pulse source for producing a switching voltage from a few hundred volts to a few kilo-volts within a few tens of ns. Inventing a simple and low-voltage E-O Q-switch is crucial for realizing a compact and low-cost actively Q-switched laser.

Among available E-O crystals, lithium niobate has been fairly popular because of its low cost and large electro-optic coefficients. When functioning as a transverse-mode amplitude modulator in two crossed polarizers, a lithium niobate crystal has a theoretical half-wave voltage of $\sim 0.66\,\mathrm{V} \times d\,(\mu\mathrm{m})/L_\mathrm{e}\,(\mathrm{cm})$ [6] at 1.064-μm wavelength, where d and L_e denote the electrode separation and the electrode length of the modulator, respectively. This voltage is, for example, ∼ 6 times less than a KDP transverse-mode amplitude modulator under the same d/L_e ratio. Recently, quasi-phase-matched (QPM) [7] nonlinear optical crystals have been found useful for electro-optic applications [8–11]. Lu et al. [8] revealed an E-O wavelength filter made from a periodically poled lithium niobate (PPLN) crystal [12]. This PPLN wavelength filter is a wavelength-dependent polarization rotator. When this E-O PPLN crystal is made into a transverse-mode amplitude modulator, its half-wave voltage is further lowered by a factor of two [13] compared to a conventional lithium niobate amplitude modulator of the same length. Due to its superior electro-optic property, an E-O PPLN crystal has been demonstrated successfully as a laser Q-switch [13]. In the first part of this paper, we further incorporate an intracavity Brewster plate into the laser cavity to greatly improve the switching voltage and output performance of the E-O PPLN Q-switched laser. With this laser configuration, we detail the theory and experiment of 1-W and 9-W diode-pumped Nd:YVO_4 lasers Q-switched by a 50–150-V E-O PPLN Pockels cell, showing excellent consistency between theory and experiment.

A QPM crystal is also known for efficient laser-wavelength conversion. For example, extracavity-pumped optical parametric generation using PPLN has been studied in the past [14, 15]. It is advantageous to access high intracavity power from a compact laser source by integrating QPM elements of the same material for both Q-switching and wavelength conversion inside a laser cavity. In the second part of this paper, we further demonstrate high-efficiency intravacity optical parametric generation from a PPLN wavelength

✉ Fax: +886-3-4252897, E-mail: yhchen@ios.ncu.edu.tw

converter in the E-O PPLN Q-switched Nd:YVO_4 laser. This demonstration reveals the advantage of monolithically integrated QPM materials for both laser Q-switching and wavelength conversion.

This paper is organized as follows. We describe in Sect. 2 the principle of an E-O PPLN laser Q-switch, discuss in Sect. 3 the experiment of an E-O PPLN Q-switched Nd:YVO_4 laser, and demonstrate in Sect. 4 efficient intracavity optical parametric generation in such a laser source. We present in the appendix the derivation of the switching voltage of an E-O PPLN laser Q-switch.

2 Electro-optic PPLN laser Q-switch

An E-O PPLN crystal consists of a stack of half-wave lithium niobate plates with their crystal axes periodically rotated about the crystallographic x axis under an electric field in the y direction. Therefore, an E-O PPLN crystal is governed by a birefringence QPM condition in which each domain of the PPLN structure behaves like a rotated half-wave phase retarder. The E-O PPLN crystal has a QPM grating period Λ given by

$$\Lambda = 2ml_c = m\frac{\lambda_0}{n_o - n_e}, \tag{1}$$

where m is an odd integer for 50%-duty-cycle domain modulation, λ_0 is the laser wavelength in vacuum, $l_c = \lambda_0/2(n_o - n_e)$ is the half-wave retardation length or the coherence length of an E-O PPLN crystal, and n_o and n_e are the refractive indices of the ordinary wave and the extraordinary wave in lithium niobate, respectively. When an electric field E_y is applied along the y direction of the PPLN crystal, the crystal axes, y and z, rotate through an angle about the x axis, given by

$$\theta \approx \frac{r_{51}E_y}{1/n_e^2 - 1/n_o^2}s(x), \tag{2}$$

where r_{51} is the relevant Pockels coefficient and the sign function $s(x) = +1\,(-1)$ along x for $+z\,(-z)$ domain orientation in the PPLN crystal. As a result, z-polarized input light rotates its polarization by an angle of $4N\theta$ at the output after traversing N domain periods in an E-O PPLN crystal. From Eq. (A5) in the appendix, the half-wave voltage is defined to be the one that rotates the laser input polarization by 90°, given by

$$V_{90^\circ} = \frac{\pi}{4}\frac{\lambda_0}{2}\frac{\sqrt{n_o n_e}}{r_{51}n_e^2 n_o^2}\frac{d}{L_e}, \tag{3}$$

for a 50%-duty-cycle, first-order ($m = 1$) E-O PPLN crystal. At 1.064-μm wavelength, the first-order E-O PPLN grating period is around 14 μm at room temperature and the half-wave voltage is $0.36\,\text{V} \times d\,(\mu\text{m})/L_e\,(\text{cm})$, which is approximately half that of a standard lithium niobate Pockels cell with an electric field applied in the z direction.

From the above, an E-O PPLN crystal can be considered as a low-voltage Pockels cell. Implementing an E-O PPLN crystal as a laser Q-switch is similar to implementing a standard Pockels cell as a laser Q-switch. Specifically, if a polarization-dependent laser gain medium, for instance, a Nd:YVO_4 crystal, is used, the E-O PPLN Q-switch can be a quarter-wave polarization rotator cascaded to a quarter-wave plate or a half-wave polarization rotator between two crossed polarizers. In the following experiment, we employed an intracavity Brewster plate in conjunction with an E-O PPLN polarization rotator to achieve a high extinction ratio between two cavity-loss (Q) states and thus an ultra-low Q-switching voltage in a diode-pumped Nd:YVO_4 laser.

3 Nd:YVO_4 laser Q-switched by an E-O PPLN Pockels cell

We fabricated a 13-mm-long, 10-mm-wide, and 0.5-mm-thick PPLN crystal with a 14-μm domain period phase matched to the first-order E-O QPM condition in Eq. (1) for 1.064-μm laser wavelength at 34.5°C. Two 400-μm-deep and 120-μm-wide trenches were cut into the PPLN $+z$ surface and sputtered with metal to form electrodes [13]. The two electrodes were parallel along the x direction and separated by 1 mm in the y direction. According to Eq. (3), the quarter-wave voltage of this E-O PPLN Q-switch is ∼ 140 V. The effective laser aperture of the E-O PPLN crystal was 0.4 mm × 1 mm in the y–z plane. Figure 1 shows the schematic of the Nd:YVO_4 laser with the E-O PPLN Q-switch. The laser gain medium was a 1-mm-long a-cut Nd:YVO_4 crystal doped with 2-at.% Nd^{3+}. The pump laser was a fiber pig-tailed diode laser radiating at 809 nm with a 2.5:1 polarization ratio. The pump side of the Nd:YVO_4 crystal was coated with a high-reflection (HR) dielectric layer with reflectance > 99.9% at 1.064-μm wavelength and an anti-reflection (AR) layer at 809-nm wavelength. The output coupler was a 20-cm radius-of-curvature (ROC) plano-concave mirror with 87% reflectance at 1.064 μm. The laser cavity length was approximately 3.8 cm. The optic axis of the E-O PPLN Q-switch was aligned with that of the Nd:YVO_4 crystal so that the laser has the highest gain when no voltage

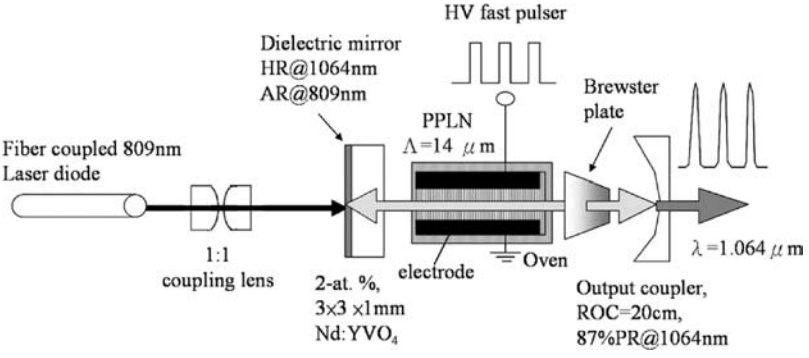

FIGURE 1 The schematic of the 1-W diode-pumped Nd:YVO_4 Q-switched laser employing an E-O PPLN Pockels cell and an intracavity Brewster plate. PR: partial reflection; other abbreviations defined in text

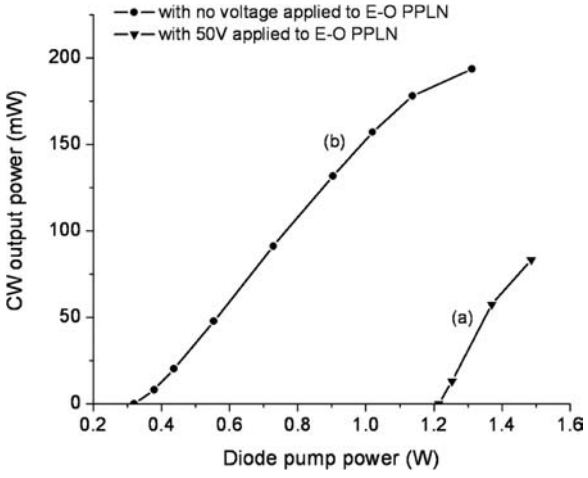

FIGURE 2 The CW output power of the Nd:YVO_4 laser system as a function of the input diode power with DC 50 V (a) and without a voltage applied to the E-O PPLN crystal (b)

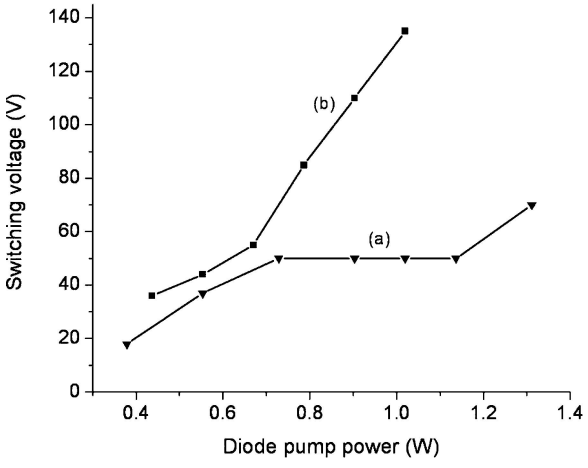

FIGURE 3 The measured minimum Q-switch voltages for various pump powers in the Nd:YVO_4 Q-switched laser with (a) and without (b) an intracavity Brewster plate

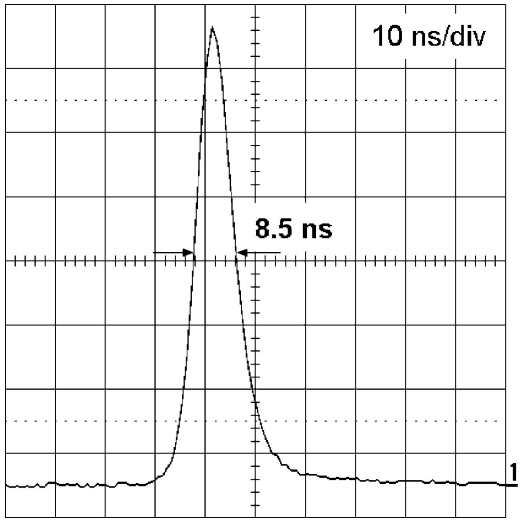

FIGURE 4 The measured Q-switched pulse from the Nd:YVO_4 Q-switched laser at 1-W pump power and 13% output coupling. The pulse width was 8.5 ns and the pulse energy was about 7.7 μJ

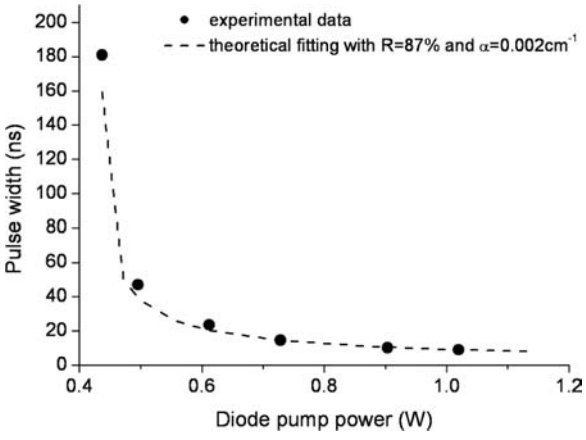

FIGURE 5 The measured pulse width versus the diode pump power. The *dashed line* is the theoretical curve

is applied to the E-O PPLN Q-switch. The purpose of the 125-μm-thick Brewster plate was to introduce more loss to light not polarized in the z direction. The E-O PPLN was installed in an oven controlled at the 34.5°C phase-matching temperature. The continuous-wave (CW) performance of the Nd:YVO_4 laser system is plotted in Fig. 2, where curve (a) corresponds to a 50-V voltage in the E-O PPLN crystal and curve (b) corresponds to no voltage in the E-O PPLN crystal. Curve (a) clearly shows a hold-off pump power of 0.9 W for the Nd:YVO_4 laser. Figure 3 shows the minimum Q-switch voltages in the E-O PPLN crystal for various pump powers (a) with and (b) without the Brewster plate inside the laser cavity. Below the minimum Q-switch voltage, no Q-switch pulse was generated from the laser. As Fig. 3 shows, the minimum Q-switch voltage is greatly reduced with the installation of the Brewster plate. This voltage reduction is even more evident at high pump power, because a Nd:YVO_4 crystal is not an ideal polarization-dependent laser gain medium for high-power operation [16]. It is apparent from Figs. 2 and 3 that with the Brewster plate in the laser cavity the PPLN Q-switch voltage can be much less than its quarter-wave voltage or 140 V.

At 1-W diode power, 1.064-μm Q-switched pulses were gradually produced from the laser system when a 50-V voltage pulse with 300-ns duration and 6.5-kHz repetition rate was applied to the E-O PPLN Q-switch. At a 100-V Q-switched voltage, we measured an 8.5-ns, 7.7-μJ Q-switched pulse from the Nd:YVO_4 laser, as shown in Fig. 4, corresponding to an average output power of 50 mW at 6.5-kHz pulse rate. We found that the amplitude fluctuation of the Q-switched pulse train was less than ±5% when the E-O PPLN Q-switch was temperature stabilized within ±0.1°C of its phase-matching temperature 34.5°C. Figure 5 shows the measured pulse width varying with the diode pump power at a 100-V Q-switch voltage. The pulse width decreased from ∼ 180 to ∼ 9 ns as the pump power was increased from 0.43 to 1 W. By using the loss coefficient in lithium niobate $\alpha = 2 \times 10^{-3}$ cm^{-1} and the upper-level lifetime = 60 μs for a 2-at.% Nd:YVO_4 crystal, we calculated the theoretical Q-switched pulse width versus pump power according to the model in Refs. [17, 18], given by

$$p_w = p_s \frac{r\eta(r)}{r - 1 - \ln(r)} \tau_c, \tag{4}$$

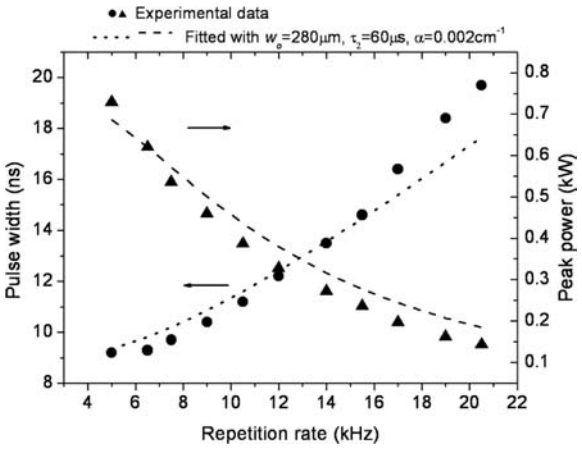

FIGURE 6 The measured laser pulse width and laser peak power versus the Q-switch repetition rate at 1-W pump power. The *dotted curve* and the *dashed curve* are the theoretical predictions

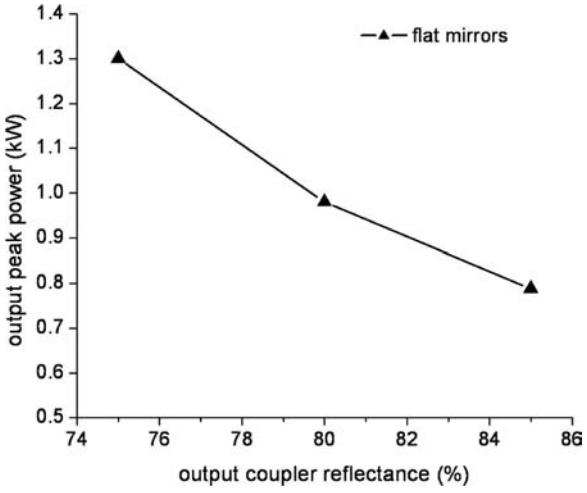

FIGURE 7 The peak output power versus the reflectance of the output coupler at 1-W pump power and 6.5-kHz Q-switch rate

with the energy-extraction efficiency $\eta = 1 - e^{-r\eta}$, where p_s is the pulse-shape function, τ_c is the cavity photon lifetime, and r is the initial population-inversion ratio just after Q-switching. The initial population-inversion ratio is a function of the CW pumping rate, laser upper level lifetime, and Q-switching repetition rate. The dashed curve in Fig. 5 shows the calculated result for the CW pump power range from 0.43 to 1.1 W at a fixed 6.5-kHz Q-switch repetition rate. The experimental curve agrees very well with the theoretical curve. To account for the observed enhanced crystal absorption originating from the high-temperature dielectric coating process under the oxygen-deficient environment [19], the assumed absorption coefficient in lithium niobate, $2 \times 10^{-3}\,\mathrm{cm}^{-1}$, in our calculation was slightly larger than its typical value of $1.5 \times 10^{-3}\,\mathrm{cm}^{-1}$ at 1.064 μm [20].

Figure 6 shows the measured pulse width and peak power versus the Q-switch repetition rate from the Nd:YVO_4 laser system at 1-W diode pump power. Following Eq. (4), we also plotted the theoretical curve of the pulse width versus repetition rate between 5 and 20.5 kHz for comparison, as shown by the dotted line in Fig. 6. It is seen that the measured pulse width was only in good agreement with the theoretical value for a repetition rate less than 16 kHz. For repetition rates higher than 16 kHz, the measured pulse width was longer than the theoretical value. The discrepancy is attributable to the slow rise time of our voltage pulse source at high pulse rates.

With reference to Refs. [17, 21], we derived the theoretical peak output power as a function of the pulse rate, given by

$$P_p = \frac{-\ln R}{8}\frac{\pi w_o^2}{\tau_c \sigma} h\nu(r - 1 - \ln r), \tag{5}$$

where h is Planck's constant, ν is the laser frequency, R is the output-mirror reflectance (0.87 in our case), $\sigma = 25 \times 10^{-19}\,\mathrm{cm}^2$ is the stimulated emission cross section of an a-cut Nd:YVO_4 crystal [22], and w_o is the laser waist radius. The dashed curve plotted in Fig. 6 shows the prediction of Eq. (5) for a repetition rate from 5 to 20.5 kHz. In plotting the theoretical curve, we have chosen $w_o = 280\,\mu\mathrm{m}$, which is approximately the waist radius deduced by imaging the 600-μm core-diameter fiber-pigtailed diode laser output to the Nd:YVO_4 crystal through a 1:1 coupling lens in our system. It is seen from Fig. 6 that the experimental peak power as a function of laser repetition rate agrees reasonably well with the theoretical value. The slightly lower experimental peak power at high repetition rates is consistent with the slightly longer measured pulse width.

It is evident from Eq. (5) that, in an actively Q-switched laser system, the peak output power P_p is dependent on the initial inversion ratio r and the reflectance R of the laser output coupler. Figure 7 shows the measured peak output power versus the reflectance of the output coupler at fixed ∼ 1-W pump power and 6.5-kHz pulse rate. In the plot, the output peak power monotonically increases from 0.8 to 1.3 kW when the reflectance of the output coupler is reduced from 85 to 75%. This result suggests that an output coupler having a reflectance $< 75\%$ is favorable for further enhancing the peak power of the current Q-switched laser system [18]. The output couplers used for plotting Fig. 7 were all flat mirrors due to the availability in our laboratory. It is interesting to note that thermal lensing in such a compact laser system was sufficient for establishing Q-switched laser oscillation.

4 QPM elements for both intracavity optical parametric generation and laser Q-switching

Intracavity nonlinear frequency conversion takes the advantage of high intracavity laser power to achieve high energy efficiency in nonlinear frequency conversion. In the following, we present intracavity optical parametric generation (OPG) from a PPLN crystal cascaded to the E-O PPLN Pockels cell in the Nd:YVO_4 Q-switched laser. In this work, for the first time to the best of our knowledge, both laser Q-switching and wavelength conversion were accomplished by cascaded QPM crystals of the same material in a laser cavity.

To demonstrate efficient intracavity optical parametric generation, we further constructed a high-power diode-pumped Nd:YVO_4 Q-switched laser system, as shown in Fig. 8, wherein an E-O PPLN Pockels cell was used for laser Q-switching and the other PPLN crystal was used for wavelength conversion. The laser gain medium was a 0.25-at.% a-cut Nd:YVO_4 crystal with a 3 mm × 3 mm laser aperture

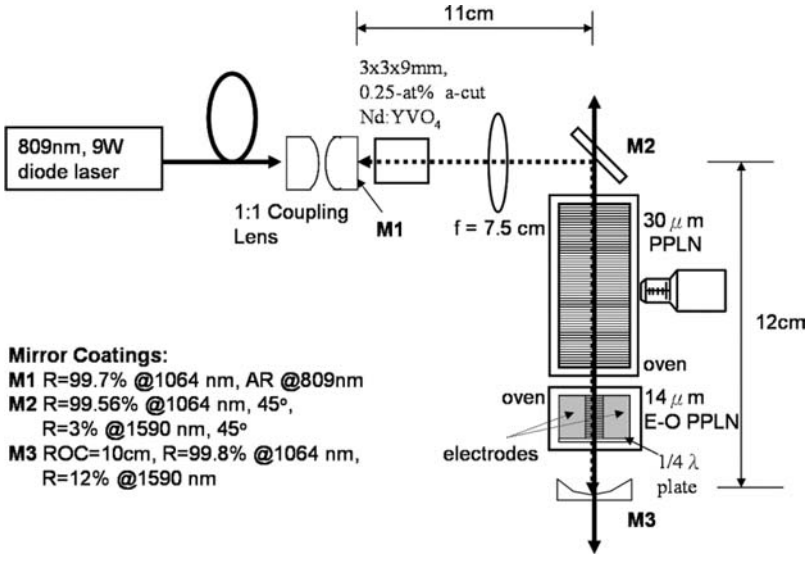

FIGURE 8 The schematic of a 9-W diode-pumped Nd:YVO_4 Q-switched laser comprising a 5-cm long, 30-μm-period PPLN wavelength converter cascaded to the E-O PPLN Pockels cell. R: reflectance; other abbreviations defined in text

and 9-mm length. The reduced Nd doping level was to avoid thermally induced fracture [23] in high-power operation. The PPLN Pockels cell in this laser system was a quarter-wave polarization rotator cascaded to a quarter-wave plate [13]. The 1.064-μm wave oscillated in a 23-cm L-folded cavity defined by the three high-reflection mirrors, M1, M2, and M3. Mirror M1 was a 99.7% high-reflection dielectric coating at 1.064-μm wavelength on the flat output surface of the 1:1 pump coupling lens. Mirror M2 was a 45° flat reflector with 99.56% reflectance at 1.064-μm wavelength and 97% transmittance at 1.59-μm wavelength. Mirror M3 was a plano-concave mirror having a radius of curvature of 100 mm and a dielectric coating with 99.8% reflectance at 1.064-μm wavelength and 88% transmittance at 1.59-μm wavelength. The 5-cm-long and 1-mm-thick PPLN wavelength converter had a grating period of 30 μm for phase matching a 1.59-μm signal wave and a 3.216-μm idler wave to a 1.064-μm pump wave at 130°C. Both end faces of this PPLN crystal were anti-reflection coated at both the 1.064-μm pump wavelength and the 1.59-μm signal wavelength. The signal and idler waves propagated in both longitudinal directions of the PPLN wavelength converter, emitting through the cavity mirrors M2 and M3. Because the 1.064-μm wave oscillates in a high-finesse resonator and pulsed operation is not effective without the PPLN wavelength converter, the Q-switched optical parametric generation resembles a cavity-dumping process for the 1.064-μm power [24]. This nonlinear dumping process is expected to produce a short OPG pulse length and a depleted 1.064-μm pulse tail comparable to the photon lifetime of the resonator.

We drove the PPLN Pockels cell with a 6-kHz, 300-ns pulse-width voltage pulse train at an amplitude of ∼ 150 V. When pumped by 9-W diode laser power, the OPG system generated ∼ 3-ns signal pulses, as shown in Fig. 9. The measured OPG threshold was near 3.8-W diode power, which is about two times the CW lasing threshold for the Nd:YVO_4 laser system in Fig. 8. Figure 10 shows the output pulse of the generated 1.59-μm signal pulse overlapped with the depleted 1.064-μm laser pulse at 9-W diode pump power. As expected, the sharp 1.59-μm signal pulse was generated at

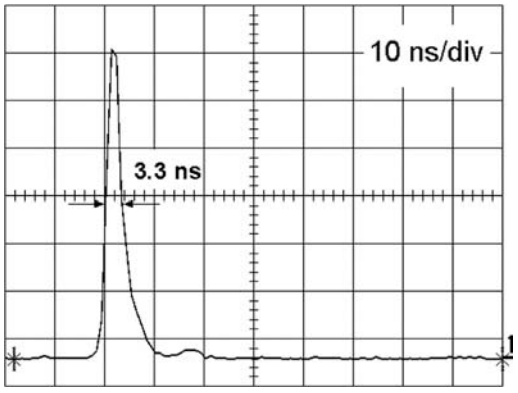

FIGURE 9 The OPG signal pulse generated from the laser system in Fig. 8 at 9-W diode pump power. The pulse width was 3.3 ns and the peak power was about 1.5 kW

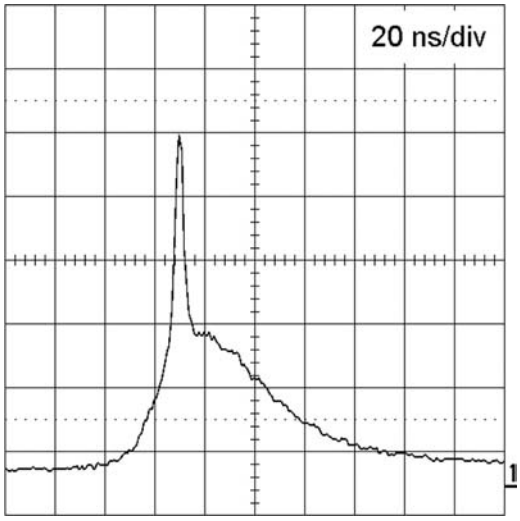

FIGURE 10 The output pulse of the generated 1.59-μm signal pulse overlapped with the depleted 1.064-μm laser pulse at 9-W diode pump power. The sharp 1.59-μm signal pulse was generated at the leading edge of the depleted 1.064-μm pulse. Note that the pulse amplitudes for the 1.064-μm wave and the 1.59-μm wave are not plotted to scale due to their different spectral transmittances at the output mirror

the leading edge of the depleted 1.064-μm pulse. Note that the pulse amplitudes for the 1.064-μm wave and the 1.59-μm wave are not plotted to scale due to their different spectral transmittances at the output mirror. Note also from the figure that the 1.064-μm pulse extends over a duration of ∼ 60 ns, which is consistent with the 1.064-μm cavity photon lifetime of ∼ 59 ns calculated from the PPLN absorption loss $\alpha = 0.002\,\mathrm{cm}^{-1}$ and those reflectance values of the mirrors given previously. At 9-W diode pump power, we measured 1.5-kW peak signal power or 30-mW average signal power at the M2 output. The signal output energy exiting M2 was about 5 μJ repeating at 6-kHz rate. With known mirror reflectance and transmittance, we deduced the intracavity average powers of 386 and 31 mW for the depleted 1.064-μm laser and the generated signal, respectively. In terms of pulse energies, the depleted 1.064-μm wave and the signal wave have intracavity pulse energies of 64.4 and 5.2 μJ, respectively. According to the Manley–Rowe relation, the generated idler wave at 3.216-μm wavelength has an intravacity pulse energy of ∼ 2.57 μJ. From the above, we obtain an energy-conversion efficiency of 11% from the 1.064-μm wave to the signal and idler waves. Figure 11 shows the plot of the OPG output pulse energy, including that in both the signal and the idler, versus the 809-nm diode pump power. The dashed curve in the plot was an exponential fit to the measured data to illustrate the exponential gain of an OPG process [15]. The signal-detection limit for our pyrodetector was about 1 μJ/pulse. To the best of our knowledge, we have achieved the lowest diode pump power for producing μJ/pulse intracavity OPG in an actively Q-switched laser.

Figure 12 shows the wavelength tuning of this intracavity OPG source as a function of the PPLN crystal temperature from 80 to 180°C. In the plot, the signal wavelengths were measured by a grating monochromator and the corresponding idler wavelengths were deduced from the frequency-conservation law in nonlinear frequency conversion. The experimental data (dots) agree very well with the theoretical curve (solid lines) calculated from the published Sellmeier equation for a congruent lithium niobate crystal [25]. The inset shows a signal spectral width of 1.2 nm at 137°C. The nm signal spectral width is fairly typical for an infrared optical parametric generator [15].

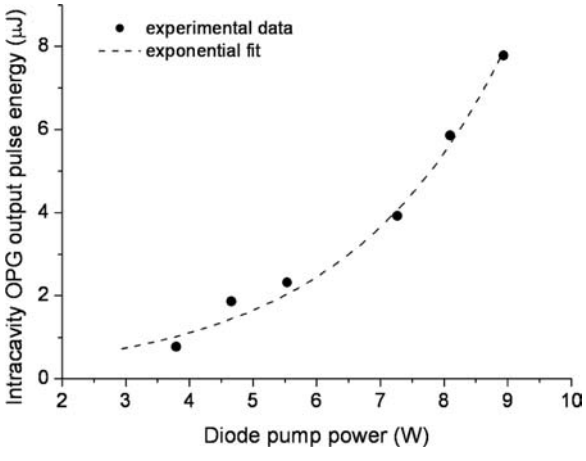

FIGURE 11 The intracavity OPG pulse energy versus the 809-nm diode pump power. The *dashed curve* is an exponential fitting curve to the measured data

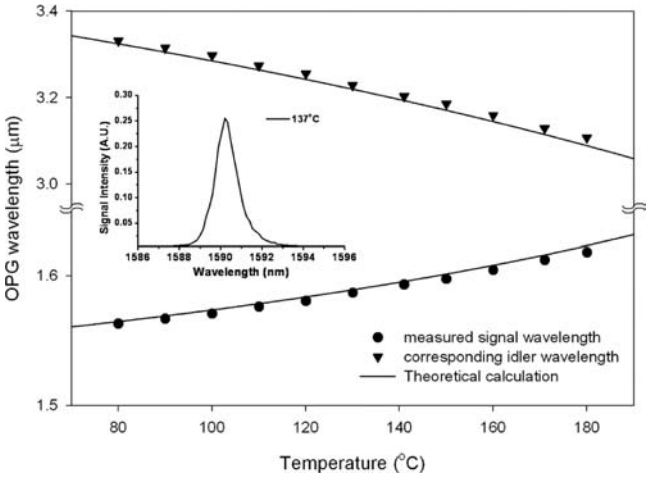

FIGURE 12 The measured signal wavelength (*dots*) as a function of the PPLN-crystal temperature from 80 to 180°C. The corresponding idler wavelengths were calculated using the frequency-conservation law in an optical parametric process. The *solid lines* were plotted according to Ref. [25]. The *inset* is the OPG signal spectrum measured at 137°C showing a spectral width of 1.2 nm

5 Discussion and conclusion

An electro-optically Q-switched laser employs a Pockels cell as a laser Q-switch. We presented in this paper an ultra-low-voltage Pockels cell for Q-switching a Nd:YVO_4 laser. This E-O PPLN Pockels cell has a theoretical switching voltage approximately half that of a conventional lithium niobate Pockels cell of the same physical dimension. By using a 13-mm-long, 14-μm-period E-O PPLN crystal and an intracavity Brewster plate, we achieved a Q-switching voltage as low as 50 V in a 1-W diode-pumped Q-switched Nd:YVO_4 laser. With this improved configuration, we have also increased the pump hold-off ratio in the low cavity-Q state by a factor of two from our previous work [13] when a 50-V Q-switch voltage was applied to the PPLN Pockels cell. When driving the PPLN Pockels cell by 100-V and 300-ns pulses at 6.5 kHz, we measured 8.5-ns-width, 0.9-kW, Q-switched laser pulses with a 13% output coupler and 1-W diode pump power. The measured 1.064-μm output pulse width and peak power as a function of pulse rate were in good agreement with theoretical predictions. The relatively low Q-switch voltage together with the demonstrated laser performance will potentially simplify the design and reduce the size of an actively Q-switched laser.

Moreover, the use of a QPM lithium niobate crystal as an E-O Q-switch could lead to the integration of many QPM electro-optic, acousto-optic, and wavelength-conversion devices on a single lithium niobate substrate for intracavity applications. In particular, nonlinear frequency conversion can take advantage of the high intracavity power in a Q-switched laser. In this paper, we also demonstrated efficient optical parametric generation from a PPLN wavelength converter cascaded to an E-O PPLN Q-switch in the Nd:YVO_4 Q-switched laser. With a 5-cm-long, 30-μm-period PPLN crystal

in a 9-W pumped Nd:YVO_4 Q-switched laser, we obtained OPG signal and idler energies of 5.2 and 2.57 μJ at 1.59- and 3.216-μm wavelengths, respectively, amounting to an intracavity energy-dumping efficiency of 11%. To the best of our knowledge, this is the first intracavity OPG achieved by using QPM crystals for both laser Q-switching and wavelength conversion.

The success in combining a PPLN wavelength converter with a low-voltage E-O PPLN Q-switched laser indicates the potential of efficient harmonic generations or optical parametric oscillations in a compact, low-cost Q-switched laser resonator. Although the non-phase-matched 532-nm light generated from the PPLN crystals in a high-power Q-switched Nd laser could induce infrared absorption [26] and photorefractive damage in lithium niobate, MgO or ZnO-doped PPLN crystals [27] have been found to resist those drawbacks. Our next research effort is to lithographically integrate PPLN wavelength converters and an E-O PPLN Q-switch in a monolithic lithium niobate single crystal for efficient intracavity nonlinear wavelength conversion.

ACKNOWLEDGEMENTS This work was supported by the National Science Council, Taiwan, under Contract Nos. NSC92-2622-L007-002 and NSC92-2811-E-007-005, and by HC Photonics Co. Ltd. under NTHU Project No. 92A0082J6.

Appendix

We present in the following the derivation of the switching voltage of an electro-optic PPLN crystal. We assume that a square-wave function of period Λ and amplitude within ± 1 along x can be represented by the Fourier expansion $g(x) \equiv \sum_{m\neq 0} G_m e^{iK_m x}$, where G_m is the Fourier coefficient of the mth-harmonic grating vector $K_m \equiv 2\pi m/\Lambda$. The dielectric modulation of a PPLN crystal with grating period Λ under an electric field E_y is therefore

$$\Delta\varepsilon(x,y,z) = -\varepsilon_0 \begin{bmatrix} 0 & 0 & 0 \\ 0 & 0 & r_{51}E_y n_o^2 n_e^2 \\ 0 & r_{51}E_y n_o^2 n_e^2 & 0 \end{bmatrix} g(x) = \sum_{m\neq 0} \varepsilon_m(y,z) e^{-im(2\pi/\Lambda)x}, \quad \text{(A1)}$$

where ε_0 is the vacuum permittivity and $\varepsilon_m(y,z)$ is the mth-harmonic Fourier coefficient of the dielectric perturbation $\Delta\varepsilon(x,y,z)$. In calculating Eq. (A1), we have neglected all the diagonal terms, because they are small compared to $n_{o,e}^2$ terms in the unperturbed dielectric tensor. This anisotropic periodic dielectric modulation causes the coupling between two electro-magnetic polarization modes with a coupling coefficient κ [28]. Assuming that the square wave $g(x)$ has a duty cycle $D \equiv l/\Lambda$, where l is the length of the $+1$ amplitude, one obtains the Fourier coefficient

$$|G_m| = \frac{2}{m\pi}\sin(m\pi D), \quad \text{(A2)}$$

and thus $\varepsilon_m(y,z)$ from Eq. (A1). With known $\varepsilon_m(y,z)$, the coupling coefficient κ is given by

$$|\kappa| = \frac{\omega}{c}\frac{n_o^2 n_e^2 r_{51} E_y}{\sqrt{n_o n_e}}\frac{\sin(m\pi D)}{m\pi} \quad \text{(A3)}$$

for mode coupling through the mth spatial harmonic. By solving the coupled-mode equations [28] with the coupling coefficient in Eq. (A3), the power-conversion efficiency of one polarization mode to the other is then given by

$$T(x) = |\kappa|^2 x^2 \mathrm{sinc}^2(Px), \quad \text{(A4)}$$

where $P^2 = \kappa^*\kappa + (\Delta\beta/2)^2$ and $\Delta\beta \equiv (\beta_o - \beta_e) - K_m$ is the wave-vector mismatch coupled to the mth spatial harmonic of the dielectric grating with β_i being the wave vector of wave i in the crystal. From Eqs. (A3) and (A4), and the phase-matching condition $\Delta\beta = 0$, one can easily derive the voltage required for coupling an initially z-polarized mode to a y-polarized mode at the output of a PPLN crystal, given by

$$V_{90^\circ} = \frac{2q+1}{2}\frac{m\pi}{\sin(m\pi D)}\frac{\lambda_0}{2}\frac{\sqrt{n_o n_e}}{r_{51}n_e^2 n_o^2}\frac{d}{L_e}, \quad \text{(A5)}$$

where $q = 0, 1, 2, 3\ldots$ is a positive integer, d is the electrode separation in y, and L_e is the electrode length in x. Here we define the lowest voltage $V_{90^\circ}\big|_{q=0}$ as the half-wave voltage, $V_{\pi,\mathrm{PPLN}}$, of an E-O PPLN crystal having a duty cycle of D and a grating period of order m.

REFERENCES

1 J.J. Zayhowski, C. Dill III, Opt. Lett. **20**, 716 (1995)
2 G.J. Friel, R.S. Conroy, A.J. Kemp, B.D. Sinclair, J.M. Ley, Appl. Phys. B **67**, 267 (1998)
3 Y.X. Bai, N. Wu, J. Zhang, J.Q. Li, S.Q. Li, J. Xu, P.Z. Deng, Appl. Opt. **36**, 2468 (1997)
4 H. Plaessmann, K.S. Yamada, C.E. Rich, W.N. Grossman, Appl. Opt. **32**, 6616 (1993)
5 T. Taira, T. Kobayashi, Appl. Phys. **34**, 4298 (1995)
6 A. Yariv, P. Yeh, *Optical Waves in Crystals* (Wiley, New York, 1984), p. 232
7 J.A. Armstrong, N. Bloembergen, J. Ducuing, P.S. Pershan, Phys. Rev. **127**, 1918 (1962)
8 Y.Q. Lu, Z.L. Wan, Q. Wang, Y.X. Xi, N.B. Ming, Appl. Phys. Lett. **77**, 3719 (2000)
9 Y.Q. Lu, J.J. Zheng, Y.L. Lu, N.B. Ming, Appl. Phys. Lett. **74**, 123 (1999)
10 N. O'Brien, M. Missey, P. Powers, V. Dominic, Opt. Lett. **24**, 1750 (1999)
11 Y.H. Chen, F.C. Fan, Y.Y. Lin, Y.C. Huang, J.T. Shy, Y.P. Lan, Y.F. Chen, Opt. Commun. **223**, 417 (2003)
12 M. Yamada, N. Nada, M. Saitoh, K. Watanabe, Appl. Phys. Lett. **62**, 435 (1993)
13 Y.H. Chen, Y.C. Huang, Opt. Lett. **28**, 1460 (2003)
14 A.C. Chiang, Y.C. Huang, Y.W. Fang, Y.H. Chen, Opt. Lett. **26**, 66 (2001)
15 A.C. Chiang, T.D. Wang, Y.Y. Lin, C.W. Liu, Y.H. Chen, B.C. Wong, Y.C. Huang, J.T. Shy, Y.P. Lan, Y.F. Chen, P.H. Tsao, IEEE J. Quantum Electron. **40**, 791 (2004)
16 Y.F. Chen, Y.P. Lan, Appl. Phys. B **74**, 415 (2002)
17 A.E. Siegman, *Lasers* (University Science Books, Mill Valley, CA, 1986), Chap. 26
18 J.J. Zayhowski, P.L. Kelley, IEEE J. Quantum Electron. **27**, 2220 (1991); **29**, 1239 (1993)
19 K.L. Sweeney, L.E. Halliburton, Appl. Phys. Lett. **43**, 336 (1983)
20 http://www.crystaltechnology.com/productdata.html (the lithium niobate crystal used in this work was manufactured by Crystal Technology, Inc.)
21 O. Svelto, D.C. Hanna, *Principles of Lasers* (Plenum, New York, 1989), Sect. 5.3
22 A.W. Tucker, M. Birnbaum, C.L. Fincher, J.W. Erler, J. Appl. Phys. **48**, 4907 (1977)

23 Y.F. Chen, Opt. Lett. **24**, 1032 (1999)
24 R. Dabu, C. Fenic, A. Stratan, Appl. Opt. **40**, 4335 (2001)
25 D.H. Jundt, Opt. Lett. **22**, 1553 (1999)
26 Y. Furukawa, K. Kitamura, A. Alexandrovski, R.K. Route, M.M. Fejer, G. Foulon, Appl. Phys. Lett. **78**, 1970 (2001)
27 D.A. Bryan, R. Gerson, H.E. Tomaschke, Appl. Phys. Lett. **44**, 847 (1984)
28 A. Yariv, P. Yeh, *Optical Waves in Crystals* (Wiley, New York, 1984), Chap. 6